IOP Conf. Series: Materials Science and Engineering **63** (2014) 012028 doi:10.1088/1757-899X/63/1/012028

Investigation of the structural and microwave dielectric properties of mechanically alloyed $Fe_{40}Co_{60}$ powders

F Otmane[1], S Bergheul[1], S Triaa[2] and M Azzaz[2]
[1]Laboratoire des Sciences Aéronautiques, Université de Blida, BP 270 Route de Soumaa, Blida, Algérie
[2] Laboratoire de Science et Génie des Matériaux, USTHB, BP 32, Bab-Ezzouar, Algérie
E-mail: fotmane-aerospatiale@univ-blida.dz

Abstract. $Fe_{40}Co_{60}$ powders were produced by mechanical Alloying (MA) route. Structural and microwave dielectric properties were investigated. Discussion of obtained results is conducted according to milling time. X-Ray powder Diffraction (XRD) shows that disordered α ($Fe_{40}Co_{60}$) solid solution of substitution with body centered cubic (bcc) lattice is formed after 2h milling. Halder Wagner analysis reveals that least grain size of 15.59 nm and residual strain up to 0.8% are reached after 60h milling. The evolution of the Voigtian mixing factors according to milling progression confirms that structural properties are governed by residual strain accumulated during high- energy mechanical alloying (Gaussian profiles). Scanning Electron Microscopy (SEM) indicates that obtained powders adopt flattened angular shapes with high surface area. Microwave measurements are undertaken on bulk samples. High values of the dielectric permittivity depicting the conductive behavior of Fe-Co powders are measured. Dielectric permittivity spectra according to milling time shift towards higher values. Enhancement of the dielectric properties is related to the developed structure after milling.

1. Introduction

Several processing methods through the application of severe plastic deformation are available. Mechanical alloying as one of the severe plastic deformation methods is a solid-state reaction process. Non-equilibrium structures such as extended solid solutions and amorphous phases and alloys with a large difference in melting temperatures of ingredients can be obtained by this method [1]. Mechanical alloying is a simple processing route at low temperature which leads to significant grain refinement opening the way to new properties. The microwave dielectric properties of nanostructured materials are very important parameters to find out the suitability of these materials for microwave applications. Iron-Cobalt alloys are soft magnetic materials and confined to applications where a small volume and high performances are critical. In this study we report on the structural and microwave dielectric properties of mechanically alloyed $Fe_{40}Co_{60}$ samples obtained at different grain sizes.

2. Experimental

Elemental powders of Fe (99.9%, 50 μm) and Co (99.9%, 10 μm) were used as starting materials in nominal composition $Fe_{40}Co_{60}$ (massive ratio). High-energy mechanical alloying was performed using a Retsch PM400 planetary ball mill equipped with hardened steel balls and vials. The powders were milled for 60 hours with a ball-to- powder mass ratio of 50:1 and a milling intensity of 360 rpm. Vial charging and all powder handling were performed under protective atmosphere of argon. Small samples of powders were taken after selected milling times for structural characterization. The microstructure of milled powders was investigated by X-ray diffraction using a BRUKER D8 ADVANCE diffractometer with CuKα radiation (λ=0.15406 nm). Milled powders were coated with epoxy resin, polished and impregnated in chemical solution [2]. Finally, powders were covered of a gold coat (some angstroms of thickness) and investigated using XL 30S FEG scanning electron microscopy. Microwave measurements of dielectric permittivity were performed for bulk samples of 13 mm in

diameter and 2 mm in thickness (cold compaction: 2GPa) using resonant cavity in association with a network analyzer (Agilent 8719ES).

3. Results and discussion

3.1. Structure and morphology observation

Figure 1 shows the changes in X-ray diffraction patterns according to milling time for the elemental and milled powders. With milling progression Co peaks completely vanish due to the diffusion of Co into the bcc(Fe) structure. Fe peaks shift to the low-angle side accompanied by a diffraction line broadening and by a decrease of the intensity caused by the decrease of grain size and by the induction of strain [3]. This result confirms that the alloying formation occurs in a solid state during the milling process.

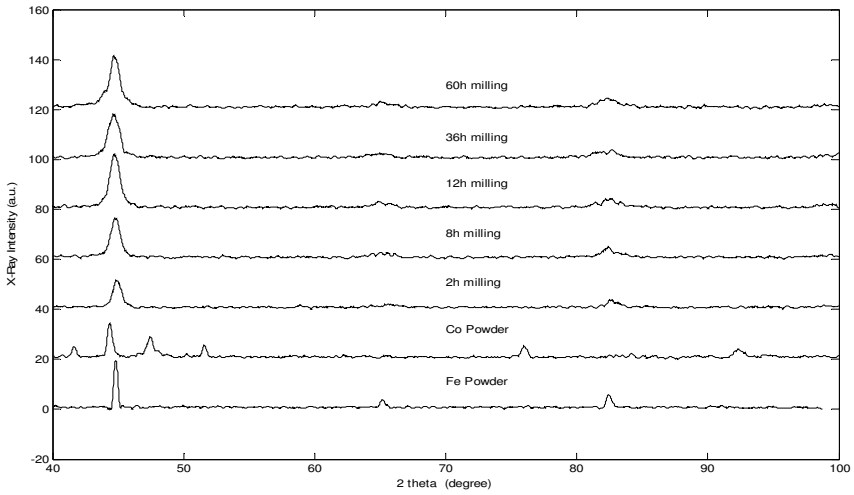

Figure 1. XRD patterns of elemental and MA $Fe_{40}Co_{60}$ powders

The Halder-Wagner approach [4] was used to fix the structural parameters at selected milling times (Figure 2). During milling the lattice parameter of Fe matrix increases gradually from 0.2856 nm to 0.2862 nm showing that Fe and Co form a solid solution. The average grain size decreases from 52.53 nm (pure Fe) to reach 15.59 nm after 60h milling (Figure 2.a). On the other hand the residual strain increases from 0.26% (pure Fe) to up 0.8% (12 h milling) due to severe plastic deformation during high-energy ball milling (Figure 2.b). After 12h milling, the residual strain decreases due to dynamic relaxation caused by extended milling [5]. Figure 2.c displays the mixing factors evolution according to milling time. Three intense peaks of XRD spectra are considered. A mixing factor ϕ is the ratio of the peak's integral breadth to its full width at half-maximum FWHM [6]:

$$\phi = \frac{w}{\beta} \tag{1}$$

with w is the full width at half-maximum (FWHM) of the XRD peak and β the integral breadth expressed as:

$$\beta = \frac{\int I(2\theta)d(2\theta)}{I_{\max}} \tag{2}$$

I is the XRD peak's intensity and 2θ the Bragg angle.

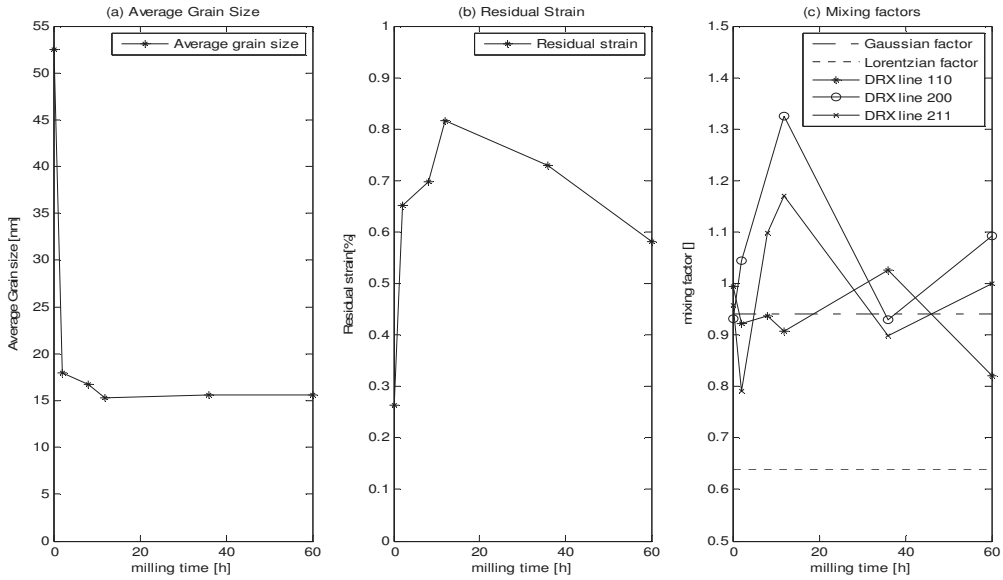

Figure 2. Structural parameters of elemental Fe and MA $Fe_{40}Co_{60}$ powders

Calculated mixing factors according to milling time in Figure 2.c are Gaussian profiles (around 0.94) showing that structural properties of MA $Fe_{40}Co_{60}$ powders are governed by internal strain induced during milling process.

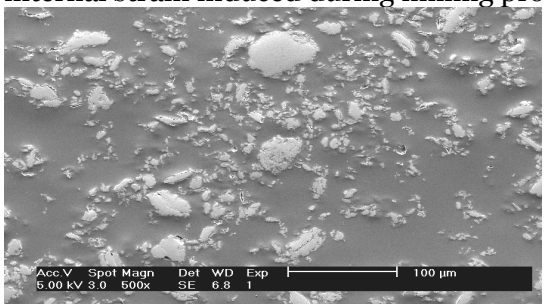

Micrograph 3.a

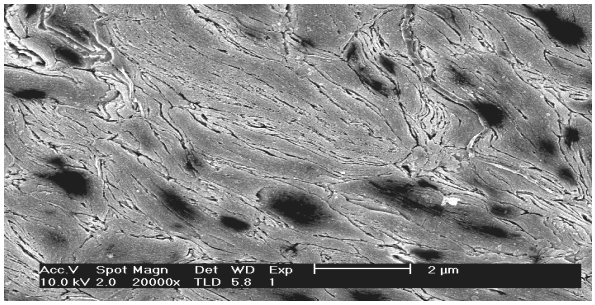

Micrograph 3.c

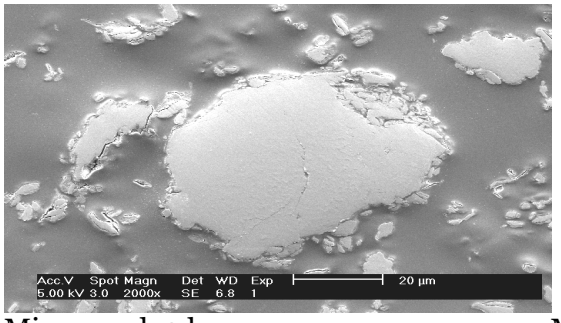

Micrograph 3.b

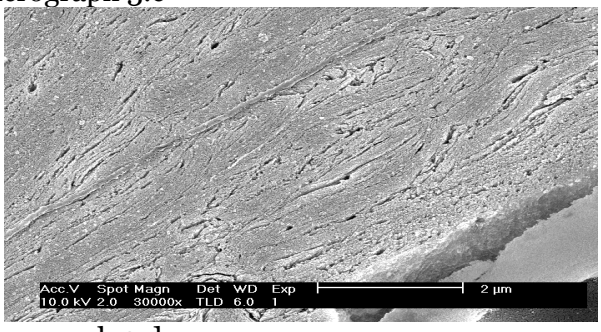

Micrograph 3.d

Figure 3. SEM observation of MA $Fe_{40}Co_{60}$ powders

First morphology observation of MA $Fe_{40}Co_{60}$ powders (12h milling) in micrograph 3.a (x500) shows a multitude of different sizes of particles. Large particles of some ten microns as well as fine particles are present. This difference of sizes is linked to the fracture and cold-welding phenomena induced during high-energy mechanical alloying [7]. Flattened angular shape with high surface area is dominant. Magnified micrograph 3.b (x2000) displays the fracture mechanism. In micrograph 3.c (x20000) we observe the lengthening lamellar aspect reflecting the ductile nature of Fe matrix (36h milling). The crystalline structure of Fe matrix is affected by the residual strain accumulated during milling and leading to order loss (micrograph 3.d).

3.2 Microwave dielectric properties

The dielectric properties such as the dielectric constant, the dielectric loss and the dielectric loss tangent are determined using the cavity perturbation technique (Figure 4). The basic principle involved in this technique is that the field within the cavity resonator is perturbed by the introduction of a dielectric sample. The resonant frequency and the quality factor of the cavity get shifted by the perturbation. The shift in the frequency is a measure of the dielectric constant and that in the quality factor gives the dielectric loss factor. According to the cavity perturbation theory the dielectric parameters are expressed as follows [8, 9]:

$$\varepsilon_r^{'} = \frac{f_0 - f_s}{2f_s}\left(\frac{V_c}{V_s}\right) + 1 \tag{3}$$

$$\varepsilon_r^{''} = \frac{V_c}{4V_s}\left(\frac{Q_0 - Q_s}{Q_0 Q_s}\right) \tag{4}$$

$$tg\delta_E = \frac{\varepsilon_r^{''}}{\varepsilon_r^{'}} \tag{5}$$

where $\varepsilon_r^{'}$ is the dielectric constant, $\varepsilon_r^{''}$ is the dielectric loss, $\overline{\varepsilon_r} = \varepsilon_r^{'} - j\varepsilon_r^{''}$ is the relative complex permittivity of the material medium and $\frac{\varepsilon_r^{''}}{\varepsilon_r^{'}}$ is usually known as the dielectric loss tangent. V_s and V_c are the volumes of the sample and the cavity resonator respectively. f_0 and Q_0 are the initial resonant frequency and quality factor corresponding to the unperturbed (empty) cavity. f_s and Q_s are the new resonant frequency and quality factor corresponding to the perturbed (charged) cavity.

Figure4.a shows the variation of the dielectric constant with milling time for the MA $Fe_{40}Co_{60}$ samples at resonant frequencies of 8.98 GHz, 9.11 GHz, 9.98 GHz and 10.38 GHz. The dielectric constant increases with milling progression for all the resonant frequencies. Accentual increase is observed between 0h corresponding to the elemental Fe phase and 12h milling due to the important fraction of grain boundaries formed during high-energy mechanical alloying process. After 12h milling the dielectric constant remains nearly the same. Grain boundaries are poorly conducting which contributes to increase the dielectric constant [10] nevertheless the dielectric constant decreases with increase in frequency at all milling times. This behavior is observed in many materials [11]. High values of measured dielectric constant are expressing the conductive nature of Fe-Co alloy.

Figure 4.b illustrates the variation of the dielectric loss according to milling progression for the MA $Fe_{40}Co_{60}$ samples at the resonant frequencies of 8.98 GHz, 9.11 GHz, 9.98 GHz, and 10.38 GHz. The dielectric loss depicts the phase lag of dipoles oscillations. The low values of dielectric loss at 0h milling are expressing the minimum energy loss when the elemental Fe interacts with microwaves. With milling progression and frequency the dielectric loss slightly increases. The reason that brings the increase behavior of dielectric loss may be attributed to the significant grain boundaries fraction and larger specific surface area present in the produced powders which increase the dissipation of microwave energy in the material medium. At 0h milling the dielectric loss tangent is between 0.2 10^{-3} and 0.4 10^{-3} which indicates that the elemental Fe sample is low loss medium. With milling progression the dielectric loss tangent is progressively improved and restricted between 7.8 10^{-3} and 15.6 10^{-3} at 60h milling (Figure 4.c) showing that the MA $Fe_{40}Co_{60}$ sample is a moderate loss medium.

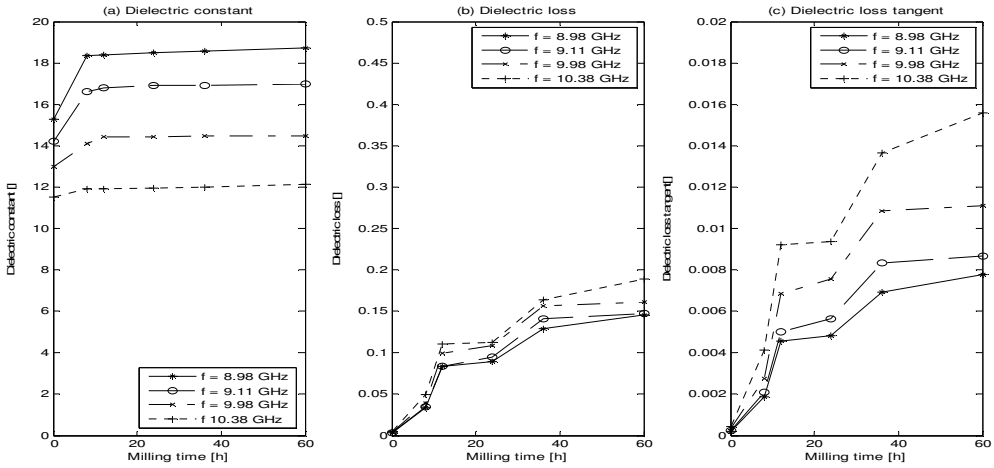

Figure 4. Dielectric parameters of elemental Fe and MA $Fe_{40}Co_{60}$ samples

4. Conclusions

The structural and dielectric properties are investigated in MA $Fe_{40}Co_{60}$ powders. XRD analysis shows that MA $Fe_{40}Co_{60}$ powders form a disordered α solid solution of substitution. Structural parameters determined using Halder-Wagner approach show that grain size decreases gradually with milling progression and reachs finally 15.59 nm. An important fraction of grain boundaries is accumulated during milling. 0.58% internal strain is fixed after 60 h milling. Calculated mixing factors of three intense XRD peaks according to milling time are Gaussian profiles confirming that structural properties of MA $Fe_{40}Co_{60}$ powders are governed by induced internal strain. The dielectric constant increased with milling progression and decreased with frequency showing that MA $Fe_{40}Co_{60}$ are moderate loss medium compared to elemental Fe. The variation of dielectric properties with milling time and resonant frequencies in the microwave range show the essential properties required for microwave applications.

5. References

[1] Koch C C 1992 Mater. Sci. Forum **88-90** 243
[2] Petzow G and Carle V 2000 Metallography Ceramography Plastography 75
[3] Moumani H, Alleg S and Greneche J M 2005 J. Alloys Compds. **386** 12
[4] Langford J I 1992 National Institute of Standards and Technology Accuracy in Powder Diffraction 110

[5] Young Do Kim, Jin Youl Chung, Jongryoul Kim and Hycongtag Jcon 2000 Mat. Sci. Eng. **A291** 17
[6] Eberhart J P 1997 Analyse structurale et chimique des matériaux Dunod
[7] Zelenakova A, Oleksakova D, Degmova J, Kovac J, Kollar P, Kusy M and Sovak P 2007 J. Magn. Magn. Mat. **316** 99
[8] Mathew K T 2002 Mat. Let. **56** 248
[9] Sheen J 2005 Measurement **37** 123
[10] Haijun Z, Zhichao L and Chenliang M 2003 Mat.Chem. Phys. **80** 129
[11] Singh P, Babbar V K and Razdan A 2000 J. Appl. Phys. **87** 4362